Crystallographic textures

G. E. LLOYD

Department of Earth Sciences, The University, Leeds LS2 9JT, England; and Centre Geologique et Geophysique, U.S.T.L., 34060 Montpellier Cedex, France

N.-H. SCHMIDT

Danish National Research Centre Riso, Postbox 49, DK-4000, Roskilde, Denmark

D. MAINPRICE

Laboratoire de Tectonophysique, U.S.T.L., 34060 Montpellier Cedex, France

AND

D. J. PRIOR

Department of Geology, University of Liverpool, P.O. Box 147, Liverpool L69 3BX, England

Abstract

To material scientists the term texture means the crystallographic orientation of grains in a polycrystal. In contrast, geologists use the term more generally to refer to the spatial arrangement or association of mineral grains in a rock. In this contribution we are concerned with the materials science definition. There are several established techniques available for the determination of crystallographic textures in rocks. It has also been realised that the scanning electron microscope (SEM) is applicable to the study of crystallographic textures via the electron channelling (EC) effect. This provides an image of mineral/rock microstructure (via orientation contrast), as well as a means of accurately indexing their crystal orientations (via electron channelling patterns, ECP). Both types of EC image result from the relationship between incident electron beam and crystal structure, and the subsequent modulation of the backscattered electron (BSE) emission signal according to Bragg's Law. It is a simple matter to switch between the two imaging modes. A related effect, electron backscattering, provides only the diffraction patterns, but has superior spatial resolution and pattern angles.

Due to crystal symmetry restrictions, there is only a limited range of ECP configurations possible for any mineral. Individual patterns can therefore be identified by comparison with the complete 'ECP-map'. The location of an individual pattern within the map area is determined by spherical angles, the exact definition of which depends on the type of fabric diagram (e.g. inverse pole figure, pole figure or orientation distribution function). Originally, these angles were measured manually. A computer program (CHANNEL) has been developed which uses a digitisation approach to pattern recognition, derives the required fabric diagrams and also constructs ECP-maps from standard crystal data (i.e. unit cell parameters etc.).

The combination of SEM/EC and CHANNEL dramatically facilitates the study of crystal textures in minerals and rocks, making statistical crystallographic analysis from individual orientations a practicality. The following example applications are considered: (1) crystal structure representation of the Al_2SiO_5 polymorph system; (2) local crystal texture relationships (epitaxial nucleation) between andalusite and sillimanite grains; (3) bulk rock crystal textures of quartzites; and (4) physical properties (e.g. elastic constants and seismic velocities) determined from bulk rock texture.

KEYWORDS: scanning electron microscopy, electron channelling, Al_2SiO_5 polymorphs, quartz, crystal fabrics, seismic properties.

Introduction

MATERIALS scientists are very specific in their use of the term texture, which they apply to the crystallographic orientation (g) of grains defined with respect to external specimen coordinates (e.g. Wenk *et al.*, 1988*a*; see also Bunge, 1982;

Mineralogical Magazine, September 1991, Vol. 55, pp. 331–345

Bunge and Esling, 1986). This relationship exists between individual grains or small groups of grains, but more usually it is taken to be the orientation distribution (OD) of many thousands of grains which characterises the whole material. In contrast, geologists are more liberal with their use of the term texture, which they apply to any description of the spatial arrangement or association of mineral grains in a rock relative to each other. Crystallographic textures in rocks are more usually referred to as fabrics or petrofabrics (e.g. Sander, 1970; Hobbs and Heard, 1986; and many others). Fortunately, cooperation on (crystal) texture analysis between geologists and materials scientists is not unknown (e.g. Wenk, 1985; Kallend and Gottstein, 1988). Any discussion therefore of mineral textures should include the crystallographic textures of individual minerals (i.e. g_1, g_2, $g_3 \ldots g_n$) and their bulk rock arrangement (i.e. OD). This is the theme of the present paper.

There are now several techniques available for the determination of crystallographic textures in materials, including minerals and rocks (e.g. Humphreys, 1988; see also many contributions in Kallend and Gottstein, 1988). These include: optical microscopy, transmission electron microscopy (involving a variety of electron diffraction based effects), X-ray techniques (e.g. texture goniometry, Laue diffraction patterns, etc.) and neutron diffraction. The use of the scanning electron microscopy (SEM) for crystal texture work on geological samples presents several specific and important advantages over classical techniques, as follows.

(1) Several different but related imaging techniques permit investigation of both specimen microstructure and crystallographic orientation.
(2) Any crystal symmetry class can be investigated, giving access to the highest Laue symmetry of the crystal being studied. This permits routine study of cubic minerals (e.g. pyrite, magnetite, chromite, garnet, etc.) and complex lower symmetry silicates (e.g. plagioclase, clinopyroxene, amphibole, etc.).
(3) The crystal orientation measurement is made on individual grains or regions of grains (e.g. subgrains, kink, bands, twins, etc.). Such an approach has several implications.

(*a*) Polyphase rocks can be easily studied (unlike X-ray and neturon texture goniometry).

(*b*) Large samples (up to several cm^2) can be studied at a high resolution of typically better than 10 μm.

(*c*) Intergranular crystallographic or spatial relationships (e.g. phase transitions, crystal plasticity, recrystallisation, etc.) are routinely determined with high precision.

(*d*) The actual crystallographic orientation and distribution in specimen coordinates (e.g. pole figures, etc.) are directly measured (unlike most other techniques).

SEM crystallographic analysis

The SEM provides two related but different methods of crystal texture analysis: electron channelling (EC), and electron backscattering (EB). Both result in essentially identical 'Kikuchi-type diffraction paterns'. However, the basic configurations of electron beam, specimen and detection systems are quite different, which must influence textural determination. EC also provides an image of the specimen microstructure (see below), but EB has superior spatial resolution and angular spread of diffraction patterns. It is not our intention to compare and contrast these two useful techniques (for details of EB see, for example, Venables and Harland, 1973; Dingley, 1988; Dingley and Baba-Kishi, 1990). In this contribution, we present examples of the potential of SEM/EC in the study of crystallographic textures in minerals and rocks.

Electron channelling. SEM/EC provides two distinct types of image, orientation contrast (OC) and electron channelling patterns (ECP). In the former, variations in image contrast distinguish individual microstructural elements (e.g. grains, subgrains, etc.) with a spatial resolution of perhaps 100 nm, although contrast difference does not reflect the exact misorientation. The latter are distinct configurations of contrast bands which are unique for a particular crystal orientation and can be obtained from a minimum area of *c.* 1 μm diameter. Both types of image result from the relationship between electron beam and crystal structure, and the subsequent modulation of the backscattered electron (BSE) emission signal according to Bragg's Law. It is a simple matter to switch between the two imaging modes, which means that the microstructure of minerals and rocks can be observed at high resolution whilst individual crystal orientations are determined. For details of the basic principles of SEM/EC, the reader is referred to Lloyd (1987). For the purposes of this contribution, only a brief outline is necessary.

The determination of mineral and rock crystal textures using SEM/EC relies on the identification and indexing of ECP's. This is achieved by recognising that there is only a limited range of pattern configurations possible owing to crystal

symmetry. Individual ECP's can be identified by comparison with an 'ECP-map' for the particular mineral crystal symmetry. The location of each pattern within the map area is fixed using spherical angles. The exact definition of these angles depends on the specific type of crystal texture diagram required (e.g. Lloyd *et al.*, 1987*a*). Inverse pole figure diagrams need only two angles to locate the ECP normal (also specimen surface and individual grain normals) within a crystal coordinate system. Pole figure diagrams need a separate pair of angles for each crystal direction measured to fix this direction in terms of a specimen coordinate system. Only three angles are necessary to define the position of the ECP/grain in terms of the orientation distribution function (ODF), which represents the complete description of the crystal texture.

The traditional method of indexing ECP's involves the construction of a spherical 'ECP-map' for each mineral, rather than each crystal symmetry class, and visual comparison between patterns and map (Lloyd and Ferguson, 1986). Construction of spherical ECP-maps is laborious and is impractical for minerals belonging to solid solution series, since each composition may require its own map. The visually-based approach to pattern indexing is also time consuming (Lloyd *et al.*, 1987*a,b*). Fortunately, a microcomputer program has now been developed which overcomes this problem.

The program CHANNEL. Schmidt and Olesen (1989) have described a microcomputer-based procedure (the program CHANNEL) to assist crystallographic analysis in the SEM. This program not only facilitates indexing of crystal orientations, but also provides a means of studying many other crystallographic aspects of rocks and minerals. The program requires the unit-cell constants (axis lengths and inter-axial angles) and positions of each atomic species in the unit cell (e.g. Smythe and Bish, 1988). The atomic positions determine the electron scattering or reflection characteristics and therefore the geometry, symmetry and intensity of the electron channelling bands in ECP-maps. The diffraction intensity is calculated by applying the expression of the crystal structure factor to each lattice plane. This approach defines the symmetry and size of any ECP-map according to the 11 possible Laue groups rather than the 32 possible point groups. This may ultimately be responsible for some loss of 'resolution' in SEM/EC analysis of certain groups. The CHANNEL program offers two types of ECP-map. Survey maps are constructed over planar surfaces and are often easier to visualise, but due to projection requirements must be viewed in section form, each section less than 60° wide. Spherical maps are constructed over spherical surfaces and consist of a series of longitudinal strips, ideally *c.* 5° in width (Schmidt and Olesen, 1989, Figs. 6 and 7*a*). Indexing of individual ECP's involves the digitisation of each pattern obtained from the SEM, followed by a computer search for the position of the pattern within the ECP-map. This position is defined by an orientation matrix from which any type of crystal fabric diagram can be derived and plotted. It is worth mentioning that although originally developed as an aid to indexing ECP's, CHANNEL is a more general research tool for crystallographic studies, capable of processing and/or producing a wide range of crystallographic information of interest to earth scientists.

Applications. The examples presented below are intended to show how SEM/EC and CHANNEL can be used in the study of crystallographic textures. We begin with the definition of a crystallographic data base, the ECP-map. In practice, this resides within the memory of the program, where comparisons with individual ECP's are made prior to the derivation of the required crystal fabric diagrams. However, the maps can be produced graphically and are significant aids to our appreciation of crystal structure. Having established a data base, we use it to study the crystallographic relationships between adjacent grains. This scale of application will perhaps prove to be the most significant for the SEM/EC technique. A second crystallographic data base (ECP-map) is used to show how SEM/EC can be used to derive whole-rock crystal textures. The significance of this approach compared with other techniques is discussed in terms of the derivation of the complete three-dimensional orientation distribution function. Finally, we show how crystal textures can be used to derive various physical properties of individual minerals and whole rocks.

Crystal structure representation

The Al_2SiO_5 polymorphic mineral system (e.g. Kerrick, 1990) consists of three main minerals: sillimanite, andalusite, and kyanite. Sillimanite and andalusite have the same orthorhombic symmetry, Laue group *mmm*, but belong to different space groups. Their crystallographic unit triangles cover a quarter of a hemisphere. In contrast, kyanite has triclinic symmetry, Laue Group -1, and its unit triangle covers the entire crystallographic sphere. Nevertheless, the crystal structures of the three polymorphs are very

similar, consisting of frameworks of chains of edge-sharing AlO_6 octahedra parallel to the *c* axis bound to each other by SiO_4, AlO_4, AlO_5, and AlO_6 polyhedra (e.g. Vaughan and Weidner, 1978).

ECP-maps for sillimanite and andalusite have been constructed using a 32 atom unit cell, involving 8 aluminium, 4 silicon and 20 oxygen atoms. The collection of the necessary atomic coordinate data to construct ECP-maps often involves considerable search. For this particular example we accessed: Burnham and Buerger (1961), Pearson (1962), Burnham (1963*a, b*), and Winters and Ghose (1979). However, the recent compilation by Smyth and Bish (1988) should improve matters considerably. Maps used to index individual ECP's should typically have between 150 and 200 active reflectors or crystal planes (Schmidt and Olesen, 1989). Survey maps are shown in Fig. 1*a,b*. The Mercator-type projection, centred on [001], used to construct the maps means that the component 'petals' do not fit perfectly together. The straight-edge termination of each 'petal' is the crystallographic basal plane (001). The ECP-maps should be equivalent to the crystallographic unit triangles, but they cover half a hemisphere. This discrepancy arises because electron diffraction effects in certain symmetry groups mean that it is possible to view an ECP from either a positive or negative position. It is therefore easier to recognise a specific pattern if the (equivalent) 'positive' and 'negative' ECP-maps are constructed. The crystallographic unit triangle can be constructed by recognising the (010) mirror symmetry plane. The orthorhombic symmetry of both minerals can then be seen in the electron channelling band structure.

The ECP-maps for sillimanite and andalusite (Fig. 1*a,b*) are obviously similar owing to their shared symmetry elements. Differences between the maps are due to differences in the structure of the two unit cells and hence of the *x, y, z* coordinate positions of the three atomic species involved. However, small changes in structure can give rise to significant differences in the ECP-maps. For example, note the different numbers of channelling bands radiating from the [001], [0$\bar{1}$0], [010] and [100] zone axes in the two maps. These must obviously lead to different channelling band elements elsewhere in the maps.

The ECP-map for kyanite should be very different to those for sillimanite and andalusite owing to its triclinic symmetry. However, kyanite possesses a similar 32 atom unit cell, although the atomic coordinates are different. A similar reflector base of 150–200 elements was also used in map construction. The calculated ECP-map for kyanite is shown in Fig. 2. It is equivalent to the crystallographic unit triangle and covers the entire crystallographic sphere. Kyanite therefore shows no 'positive' and 'negative' effects in its ECP's. Careful examination of the principal crystal planes [i.e. (100), (010) and (001)] fails to reveal any obvious symmetry elements. Furthermore, although the [010] and [0$\bar{1}$0] zone axes are apparently of the same form, the triclinic symmetry means that they only have an inversion relationship, as their simulated ECP's clearly reveal (Fig. 3*a,b*). The same applies to the [100], [$\bar{1}$00] axes and the [001], [00$\bar{1}$] axes (Fig. 3*c–f*).

Local crystal texture relationships

The ECP-maps derived in the previous section can obviously be used to determine crystal fabrics (about which we know practically nothing) for the Al_2SiO_5 polymorph minerals. They can also be used to investigate the relationships between the three polymorphs. This could be very revealing because although their phase diagram (e.g. Day and Kumin, 1980; Kerrick, 1990) suggests they should occupy mutually exclusive geological environments, two (or sometimes all three) may occur in the same rock. This is usually explained in terms of difficulties inherent in the slow kinetics of the transformation reactions in the Al_2SiO_5 system, consequent upon the slight differences in Gibbs free energy between the three phases (e.g. Putnis and McConnell, 1980). However, it is possible that one polymorph can be transformed into another by a mechanical process similar to twinning mechanisms or martensitic transformations (Rao and Rao, 1978). Indeed, Doukhan *et al.* (1985) have recognised experimentally the strain-assisted polymorphic phase transformation of sillimanite into kyanite. It appears that dislocation core structures are strongly affected by both the temperature and mean pressure of deformation, resulting in increased flow stress. Under high compressive stress, these dislocation cores dissociate to create the preferred nucelation sites of kyanite.

Strain-assisted phase transformation is perhaps especially favoured between sillimanite and andalusite, which are crystallographically very similar. However, experimental deformations by Doukhan *et al.* (1985) failed to reveal nucleation of either of these two phases within the other. They therefore concluded that they had not observed clear evidence for the natural occurrence of polymorphic strain-induced phase transformations in the Al_2SiO_5 system. In this section, we present evidence that such phase transformations may occur.

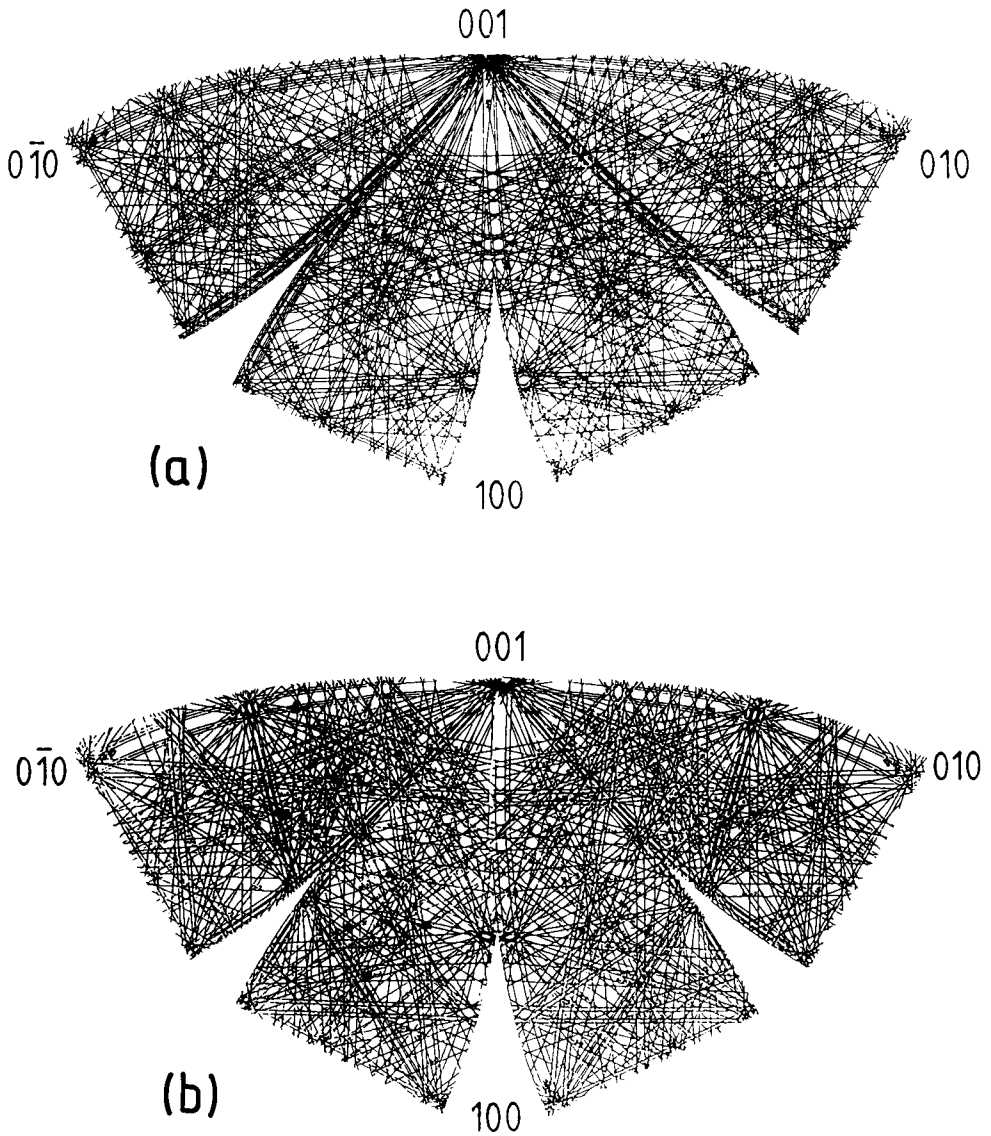

FIG. 1. Survey ECP-maps constructed using CHANNEL for (*a*) sillimanite and (*b*) andalusite, based on a 32 atom unit cell. The Mercator-type projection, centred on [001], used to construct the maps, means that the component 'petals' do not fit perfectly together. The straight-edge termination of each 'petal' is the crystallographic basal plane.

Fig. 4*a* is an orientation contrast image of sillimanite and andalusite from the aureole of the Ross of Mull granite, Scotland. The assemblage has developed through sequential polymorphic transitions from regional kyanite, through andalusite to sillimanite (A. C. Barnicoat, pers. comm., 1990). The sillimanite 'plates' appear to have nucleated in contact with the andalusite, which suggests that some structural relationship exists between the two polymorphs. This situation is ideal for investigation using ECP's and CHANNEL. ECP's from adjacent sillimanite and andalusite grains are shown in Fig. 4*b,c*. Although obviously different, both patterns do contain a similar, bright channelling band along their left margin. Simulations of these ECP's are shown in Fig. 4*d,e*. The sillimanite orientation was indexed close to [511], whilst the andalusite orientation was indexed close to [1$\bar{5}$1]. The apparently similar channelling bands were identified as the silli-

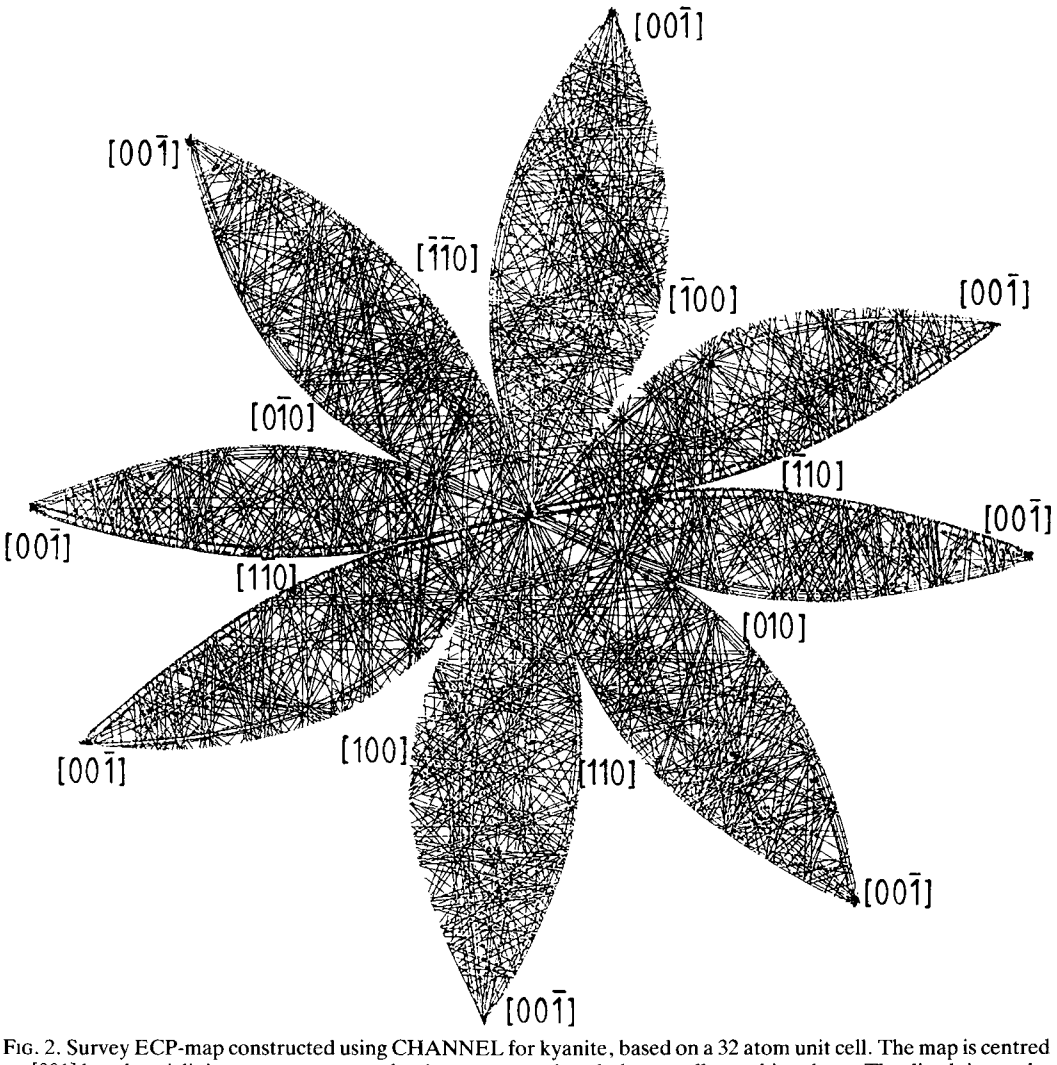

FIG. 2. Survey ECP-map constructed using CHANNEL for kyanite, based on a 32 atom unit cell. The map is centred on [001] but the triclinic symmetry means that it must cover the whole crystallographic sphere. The distal tips to the component 'petals' therefore represent the single [00$\bar{1}$] direction.

manite and andalusite basal planes, consisting of the (002), (004) and (006) reflections (although the latter is not present in the current CHANNEL reflector base for andalusite).

The crystallographic relationship between these two grains can be established by plotting the various crystal texture diagrams. The inverse pole figure diagram (Fig. 5*a*) shows that the two patterns are 90° apart. More significantly, the {001} pole figures are almost identical (Fig. 5*d*), but the positions of the [010] and [100] axes (as well as the sillimanite [511] and andalusite [1$\bar{5}$1] grain-normal crystal axes) are interchanged (Fig. 5*b,c,e* and *f*). The two grains are therefore related by a 90° rotation about the [001] axes, within the (001) basal planes. The crystal lattice *d*-spacings (in nm) for the basal plane reflectors are

sillimanite:	0.2889	0.1444	0.0963
andalusite:	0.2779	0.1389	—

which represent close approximations. Furthermore, the two grains have almost identical {110} pole figures (Fig. 5*g*) and hence the (110) and (1$\bar{1}$0) planes must also be coincident (but interchanged). The crystal lattice *d*-spacings for these planes are sillimanite 0.5362 nm, and andalusite 0.5551 nm.

These observations support the original inter-

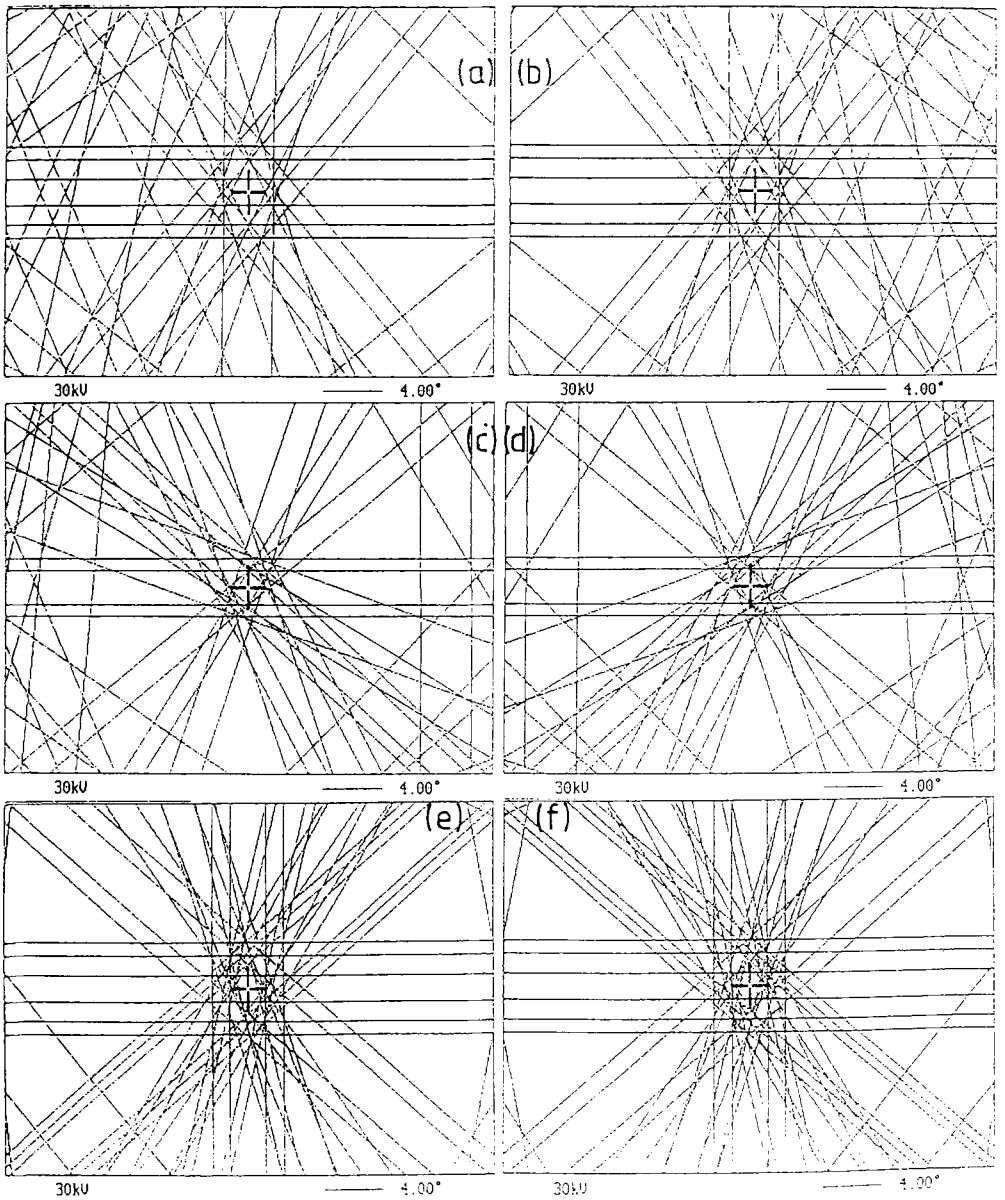

FIG. 3. Simulated ECP's for kyanite produced by CHANNEL to show the lack of symmetry in the principal crystal axes directions: (*a*) [010]; (*b*) [0$\bar{1}$0]; (*c*) [100]; (*d*) [$\bar{1}$00]; (*e*) [001]; and (*f*) [00$\bar{1}$]. In (*a*)–(*d*) the [001] axis is viewed horizontally towards the right, whilst in (*e*) and (*f*) the [010] axis is viewed horizontally towards the right.

pretation that some form of crystallographic relationship exists between the grains. We suggest that the nucleation, orientation and growth of the sillimanite has been controlled by the parental andalusite grain (001) and ⟨110⟩ planes in an epitaxial or coincident site lattice arrangement. Such control could be strain induced, according to the specifications suggested by Doukhan *et al.* (1985).

Bulk rock crystal texture

Perhaps the most obvious use of SEM/EC is in the determination of crystal fabrics of deformed

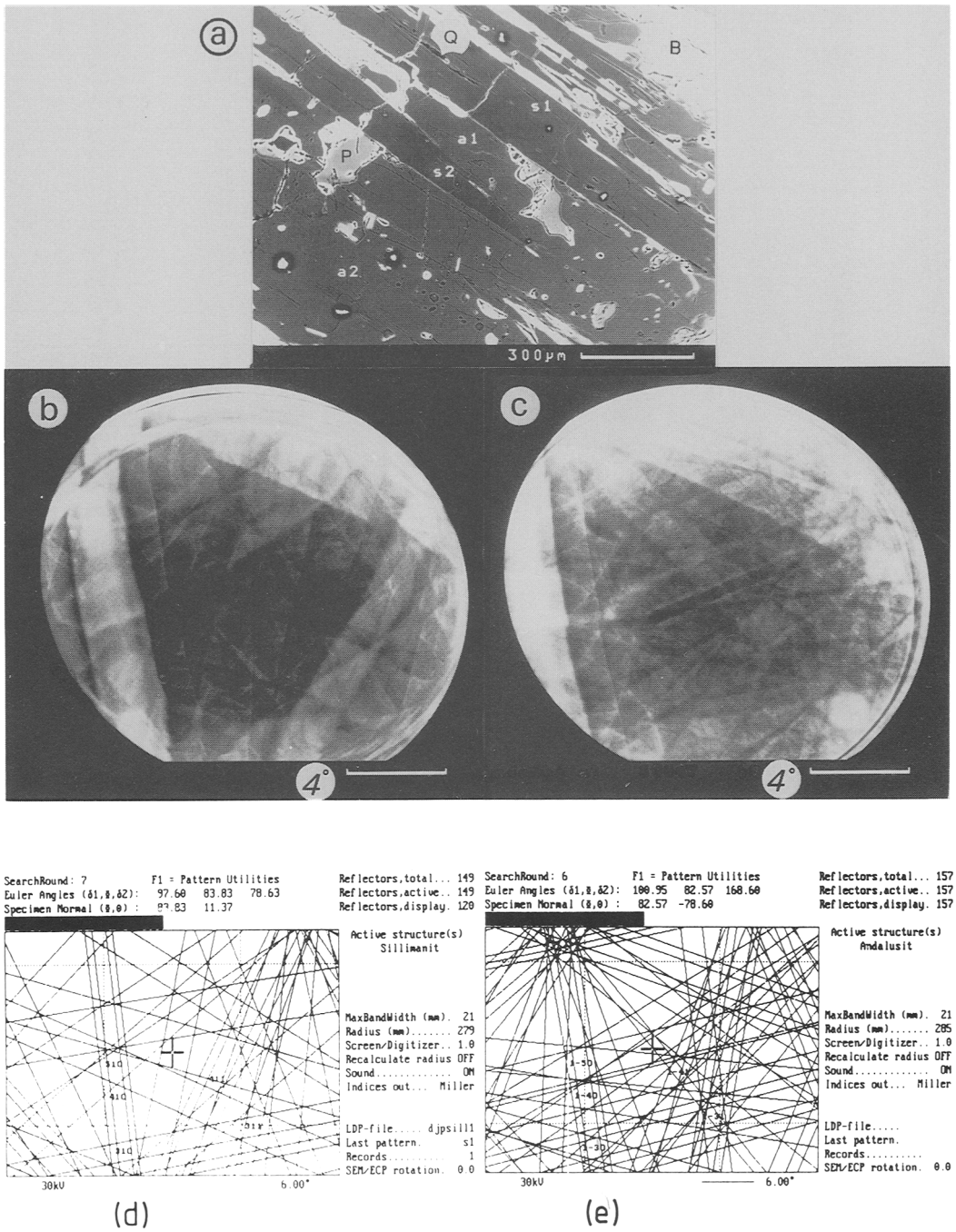

FIG. 4. Example use of ECP's and CHANNEL to determine crystallographic relationships between sillimanite and andalusite grains. See text for details. (*a*) SEM/EC orientation contrast image of sillimanite 'plates' (s1–2) in andalusite (a1–2); other minerals present are biotite (B), plagioclase (P) and quartz (Q). (*b*) and (*c*) ECP's from adjacent sillimanite and andalusite grains (s1 and a1). Note the similar bright channelling band present along the left margin in both patterns. (*d*) and (*e*) Simulated ECP's for grains s1 and a1. The former is indexed close to [511] and the latter close to [$1\bar{5}1$]. The similar channelling bands are identified as the crystal basal (001) planes.

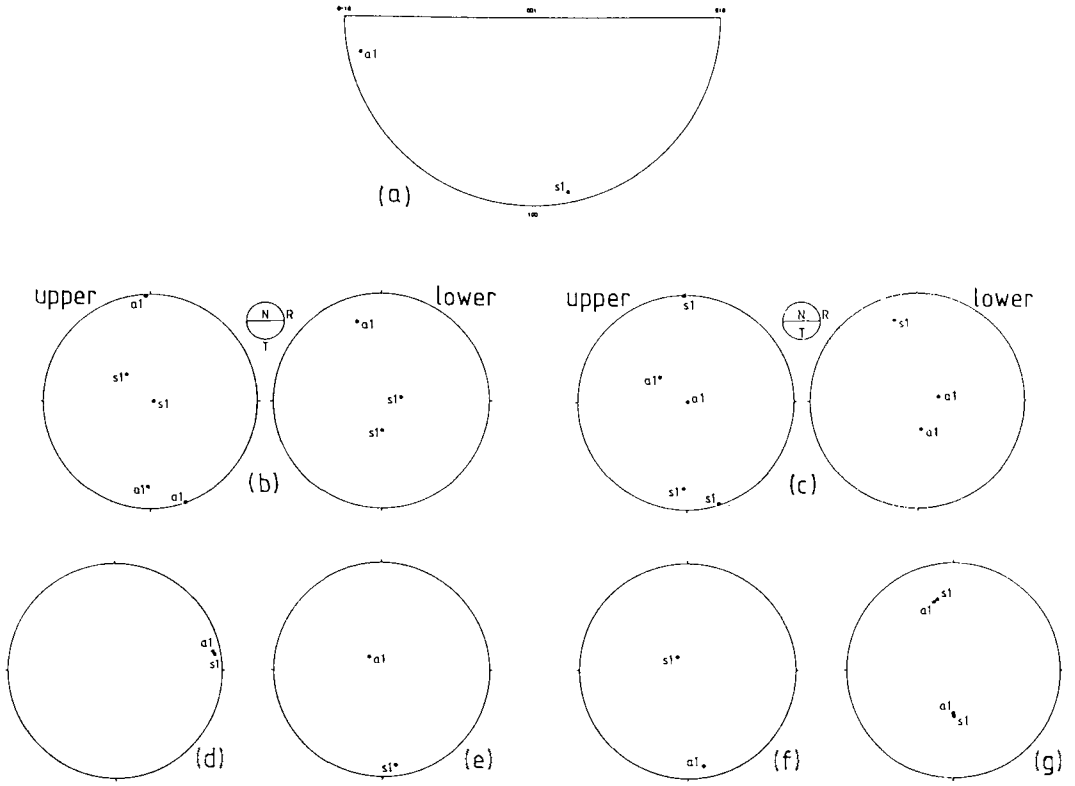

FIG. 5. CHANNEL-derived crystallographic relationships between the sillimanite (s1) and andalusite (a1) grains shown in Fig. 4. See text for details. (*a*) Inverse pole figure. (*b*) Pole figure for sillimanite pattern normal crystal axis, close to [511]. (*c*) Pole figure for andalusite grain normal crystal axis, close to [$1\bar{5}1$]. (*d*)–(*g*) Respectively [001], [010], [100] and [110] crystal axis pole figures for andalusite and sillimanite.

rocks. However, before the advent of CHANNEL, the labour involved in photographing and indexing the numbers of individual ECP's necessary for statistically meaningful bulk fabric determinations made use of the technique impractical. For example, Lloyd *et al.* (1987*a*,*b*) considered only 100 quartz grains in their original ECP studies and each pattern required up to ten minutes for measurement of the various sets of spherical angles required to construct the different fabric diagrams. This was unfortunate, because in principle the technique allows the determination of the complete crystal fabric of any mineral, rather than the specific fabrics of certain minerals (such as quartz, calcite, olivine, etc.), in both mono- and poly-mineralic rocks. In contrast, the versatility of SEM/EC has always made it ideally suited to the investigation of local crystal fabrics and microstructures (e.g. Lloyd and Ferguson, 1986; Christianssen, 1986; Ferguson *et al.*, 1987; Lloyd and Knipe, 1990). Fortunately, it is now possible using CHANNEL to index relatively quickly the large numbers of ECP's required for bulk-rock fabric analysis.

Pole figure diagrams. Fig.6 shows a range of bulk-rock pole figure diagrams constructed from 382 grains in the same Tongue quartzite specimen considered by Lloyd and Ferguson (1986) and Lloyd *et al.* (1987*a*,*b*). It required on average less than one minute to digitise and orientate successfully each ECP with the aid of CHANNEL. (The main delay now is associated with the photographic recording of each pattern, but the use of SEM frame stores and video-recorders will markedly shorten recording times.) The orientation matrix derived via CHANNEL provides all the necessary data to construct each fabric diagram for either hemisphere of projection. The pole figures are in excellent agreement with those determined by X-ray texture goniometry (see Lloyd *et al.*, 1987*b*, Fig. 2).

X-ray texture goniometry is still preferred for absolute bulk fabric analysis, particularly for rocks where the fabric is weak and several thousand grain orientations may be required to

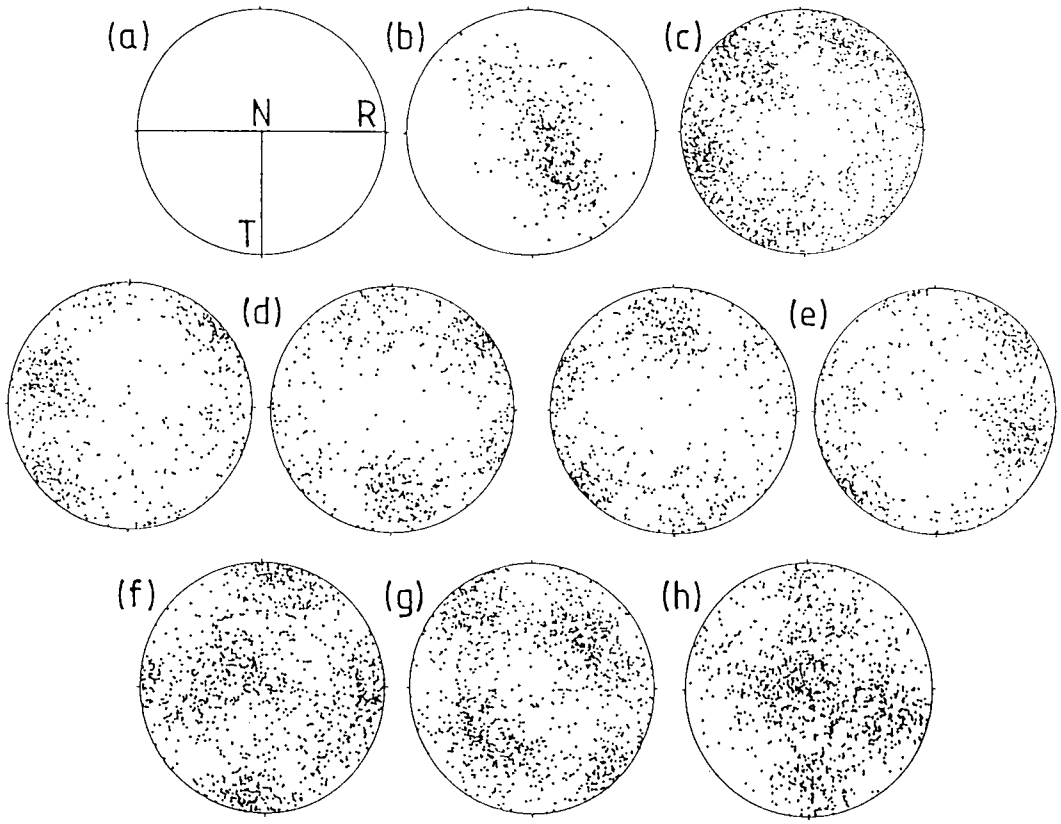

FIG. 6. Pole figure fabric diagrams derived from 382 grains in Tongue quartzite and indexed using CHANNEL. (*a*) Specimen orientation coordinates: R, reference extension (tectonic X) direction; N, specimen normal (tectonic Y) direction; T, mutually orthogonal (tectonic Z) direction. (*b*) *c*-axis (382 vectors plotted). (*c*) *m*-axes (1146 vectors). (*d*) Negative *a*-axes $\{11\bar{2}0\}$, upper (left) and lower (right) hemispheres (578 and 568 vectors respectively). (*e*) Positive *a*-axes $\{\bar{1}120\}$, upper (left) and lower (right) hemispheres (568 and 578 vectors respectively). (*f*) *r*-axes (1146 vectors). (*g*) *z*-axes (1146 vectors). (*h*) $\{10\bar{1}2\}$ axes (1146 vectors).

characterise it accurately. However, it must be remembered that SEM/EC allows each orientation in a fabric to be identified with a particular grain and the position of this grain within the general rock microstructure. X-ray goniometry is also commonly unsuitable for polymineralic rocks and is restricted to certain grain sizes. Furthermore, SEM/EC recognises specific crystallographic relationships which other techniques ignore. For example, ECP's are capable of distinguishing between the two *a*-axes (Lloyd and Ferguson, 1986; Lloyd *et al.*, 1987*a*): $\{11\bar{2}0\}$ and $\{\bar{1}120\}$, the negative (left) and positive (right) trigonal prisms (Frondel, 1962). Unfortunately we cannot say which is which for a particular pattern due to the enantiomorphism ('handedness') of quartz (Donnay and Le Page, 1978) and the consequences of Friedel's law, by which diffraction induces an apparent centre of symmetry (chirality). In principle it should be possible to distinguish right- and left-handed quartz grains from ECP's due to the breakdown of Friedel's Law across $(1\bar{1}00)$ planes (e.g. Faivre and Le Goff, 1979). This results in differences in channelling intensity asymmetry of equivalent Bragg reflection planes on either side of these planes. Although we believe that we may have observed these (very subtle) differences in the spherical ECP-map for quartz constructed by Lloyd and Ferguson (1986, Fig. 5), they are not likely to be visible in individual ECP's. Olesen and Schmidt (1990) concluded that in practical ECP microscopy it is not possible to distinguish right- and left-handed quartz grains. SEM/EC nevertheless recognizes different *a*-axes and therefore two distinct pole figure diagrams can be constructed (Fig. 6*d*,*e*). However, due to the strict angular relationships between the 6 *a*-axis

directions within the crystal basal plane, the upper hemisphere $+a$ pole figure must be equivalent to the lower hemisphere $-a$ pole figure (and vice versa). This relationship is clearly shown in Fig. 6*d,e*.

The distinction between the two *a*-axis forms means that there must also be two crystal *m*-axes: a 'positive' $\{10\bar{1}0\}$ form and a 'negative' $\{\bar{1}100\}$ form. The distinction is much less obvious but clearly exists, particularly in the configuration of the $(11\bar{2}0)$ and $(\bar{1}\bar{1}20)$ crystal planes which pass through one or other of the two axes. The fact that quartz has trigonal symmetry also implies that adjacent *m*-axes are not identical. The implications for quartz petrofabric analyses are unknown, but in future we should perhaps also present two *m*-axis pole figures in petrofabric studies (although we do not do so in this contribution).

CHANNEL allows any crystal axis pole figure to be plotted. It is as easy to construct, for example, a $\{10\bar{1}2\}$ pole figure (Fig. 6*h*), as it is a *c*-axis pole figure. Such fabric diagrams are unusual but may be of interest since we can now observe the orientation changes which occur throughout the whole crystal structure. In this example, the $\{10\bar{1}2\}$ axis shows a distinct 'cross-girdle' fabric pattern often associated with *c*-axis fabrics (although the *c*-axis fabric for this particular quartzite is a single girdle). The asymmetry shown by this fabric ('top' towards the left or NW) is consistent with the sense of shear (overthrusting) in the region from which the rock originates (Lloyd *et al.*, 1987*a*).

Determination of the true ODF. A particular advantage of SEM/ECP crystal texture analysis is that it is possible to derive directly the complete ('true') ODF (e.g. Wenk *et al.*, 1988*b*),

$$f(g) = f^{+}(g) + f^{-}(g) \geq 0$$

where $f^{+}(g)$ and $f^{-}(g)$ are series of even and odd order spherical harmonics. Usually, only the even coefficients can be determined directly via pole figures measured by X-ray texture goniometry. Complex mathematical manipulations are then required to simulate the true ODF, but $f^{+}(g)$ often contains physically meaningless negative areas and 'ghost' orientations. For example, an ambiguity of up to 30% may arise due to a partial loss of correlation between poles belonging to the same crystal grain (Wenk *et al.*, 1988*a*). However, the orientation matrix derived by CHANNEL from each ECP defines exactly the crystal orientation of the associated grain in terms of specimen geometry. To illustrate this, we have derived the various coefficients (order of expansion L = 22) and the associated even, odd and true ODF's for the Tongue quartzite described above, using ECP's from 382 grains. We emphasise that the ODF represents the best available description of the bulk texture because it provides an estimation of the entire grain-orientation population based on the (small?) sample of individual elements actually collected. The function considers both densely and sparsely populated regions, either or both of which may be significant in any textural interpretation.

Fig. 7 is the same section ($\phi_1 = 130°$) through the three-dimensional ODF space derived respectively from the even, odd and true coefficients. This section plane contains the maximum orientation density for this particular crystal texture and therefore represents the simplest opportunity for comparing and contrasting the three textures derived. There is very good agreement between the even ODF and the true ODF, although the latter has more intense peaks (up to 50% higher density) and no negative regions. The odd ODF contains significant negative regions and much reduced peaks. It therefore appears for this rather strong texture that the even ODF provides a good indication of the distribution of crystal orientations but rather underestimates the intensity.

The ODF coefficients are normally used to calculate pole figures and inverse pole figures presented in most studies involving X-ray goniometry. We have therefore used the ODF to derive contoured pole figures (Fig. 8*a*) for comparison with the 'discrete data' pole figures determined from ECP's (Fig. 6). The agreement is excellent. We have also used the true ODF to calculate inverse pole figures (Fig. 8*b*) for the lineation and inferred shear directions. These diagrams clearly show that although the even ODF is a close approximation of the true ODF for this particular specimen, there are some significant differences. In particular, the even ODF has a 60° symmetry in the inverse pole figures, whereas this is absent in the true ODF inverse pole figure (120° symmetry and a single maximum). The true ODF inverse pole figures suggest that the lineation direction (X) is off-set from an *m*-axis, while the inferred shear direction coincides with a maximum in the *a*-pole figure and is parallel to a negative *a*-axis. This simple example suggests that previous studies of quartz crystal textures using X-ray goniometry may involve considerable (up to 60°) errors in the determination of specific directional components.

Elastic and seismic properties. The elastic stiffness constants for the Tongue Quartzite can be calculated from the individual grain orientations determined from ECP's using the Voigt average given by

$$C_{ijkl} = \left(\sum_{i}^{n} C'_{ijkl}\right)/n$$

where C_{ijkl} is the elastic stiffness tensor of the aggregate, C'_{ijkl} is the single crystal elastic stiffness tensor which has been rotated to the grain orientation in specimen coordinates, and n is the number of grains. Alternatively, we can calculate the elastic properties by using the continuous ODF to average over all possible orientations within the asymmetric unit defined by the crystal and specimen symmetry, or calculated from the ODF coefficients of the harmonic method (Wenk *et al.*, 1988*b*). In the case of triclinic crystal and specimen symmetry the integration is given by Bunge (1985),

$$C_{ijkl} = \int C'_{ijkl}\, f(g)\, dg$$

$$\text{in which, } dg = (1/8\pi^2)\sin\Phi\, d\phi_1\, d\Phi\, d\phi_2$$

where f(g) is the ODF and ϕ_1, Φ, ϕ_2 are the Euler angles defined by Bunge (1982). By numerical calculation we have verified that only constants of the ODF up to the 4th order of the even function are required. This is because elasticity is a fourth order centrosymmetric tensorial property. Although this result has few practical implications for the calculation of elastic properties from individual measurements, it is of great importance for diffraction-based texture measuring techniques. In texture goniometry only the even part of the ODF can be directly determined by the inversion of pole figures in the harmonic method. The odd function can only be estimated by assumption. The order of the even function determined by the harmonic method is directly proportional to the number of pole figures measured. Thus, if we only require the fourth order of the even function we can greatly reduce the amount of pole figure measurements. We have calculated the elastic properties (Table 1) for the Tongue quartzite using the above integration technique.

The seismic P-wave velocities (v_p) for a large number of propagation directions in three dimensions can be derived from the elastic constants by solving the Christoffel equation,

$$\det|C_{ijkl}X_jX_i - \delta_{ik}\,pV^2| = 0$$

where X is the propagation direction, p is the density, δ_{ik} is the Kronecker delta, and V is one of the three seismic velocities Vp, Vs_1, or Vs_2 (Mainprice, 1990). The Vp properties of Tongue quartzite show a strong anisotropy coefficient, $A = (V_{max.} - V_{min.})/V_{max.}$ of 11% (Fig. 9*a*). The maximum velocity correlates well with the maximum intensity in the z-pole figure (Fig. 9*b*). This is in agreement with quartz single crystal data, where the fastest propagation direction is parallel to the z-pole (Fig. 9*c*). The Vp properties have a relatively smooth distribution compared to the pole figures. This is due to the fourth-order tensorial nature of elastic (seismic) properties and the much higher order of crystallographic proper-

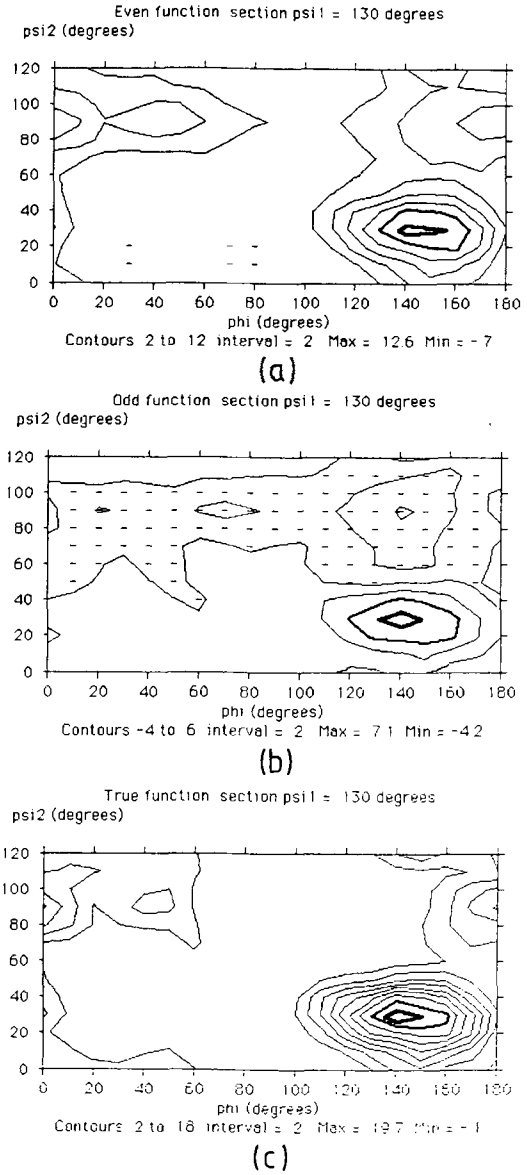

FIG. 7. Example use of SEM/EC in the derivation of the coefficients of the true orientation distribution function (ODF) for Tongue quartzite. The diagrams represent an individual section plane ($\phi_1 = 130°$) through the three-dimensional ODF space. (*a*) Even ODF. (*b*) Odd ODF. (*c*) True ODF.

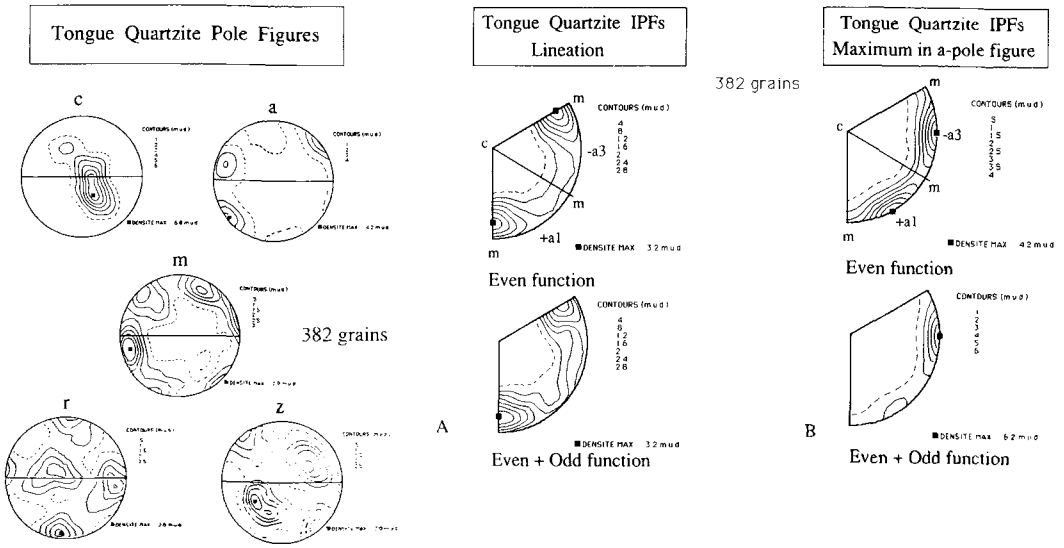

FIG. 8(*a, left*). Contoured pole figures derived from the true ODF calculated from 382 ECP's. Contours are of multiples of uniform density (m.u.d.). (*b, centre and right*) Comparison of inverse pole figures derived from the even and true ODF's for the specimen lineation (offset from an *m*-axis) and inferred shear (parallel to a negative *a*-axis) directions. Note that the even ODF results in apparent 60° symmetry (about the central *c* : *m* plane), whereas the true ODF indicates 120° symmetry and single maximum. Contours in multiples of a uniform density (m.u.d.).

ties (e.g. plasticity) which require at least an eighth order description in spherical harmonics.

Conclusions

The scanning electron microscope (SEM) electron channelling (EC) technique has been for some years a potentially powerful method for studying crystallographic textures in rocks and minerals. SEM/EC allows high-resolution images (orientation contrast) of specimen microstructure to be correlated directly with crystallographic orientation (via electron channelling patterns). This approach is suited to the study of both 'local' and 'bulk' crystal textures in most (all?) minerals and rocks. The development of the computer program CHANNEL means that the potential of the technique can now be fulfilled. The program facilitates SEM/EC investigations by allowing: (1) construction of ECP-maps for any mineral composition; (2) rapid indexing of crystal orientation from ECP's; and (3) presentation of results as crystal fabric/texture diagrams.

Acknowledgements

We thank our fellow 'fabricators' (particularly Martin Casey, Flemming Christianssen, Andy Farmer, Colin Ferguson, Brett Freeman, Rob Knipe, Rick Law, Niels Olesen and Stefan Schmid) for their interest, help and encouragement during the development of the techniques and procedures described here. Ian and Carol McNulty provided computational facilities (G. E. L.). Andy Barnicoat, Kate Brodie and Ernie Rutter made valuable comments on an earlier version of the manuscript. Financial and logistical support were provided by: U.K. N.E.R.C. and French C.N.R.S.; the Universities of Birmingham, Leeds, Aarhus and U.S.T.L. Montpellier; and the Danish National Research Centre.

TABLE 1. Elastic constants C_{ij} (in mbars) for Tongue quartzite derived from the coefficients of the true (even plus odd) orientation distribution function determined via ECP analysis.

0.9264	0.1071	0.0759	0.0119	-.0082	0.0467
0.1071	0.9013	0.0820	-.0323	0.0113	0.0208
0.0759	0.0820	1.0530	-.0081	-.0149	-.0457
0.0119	-.0323	-.0081	0.5155	-.0333	0.0047
-.0082	0.0113	-.0149	-.0333	0.5202	-.0041
0.0467	0.0208	-.0457	0.0047	-.0041	0.4835

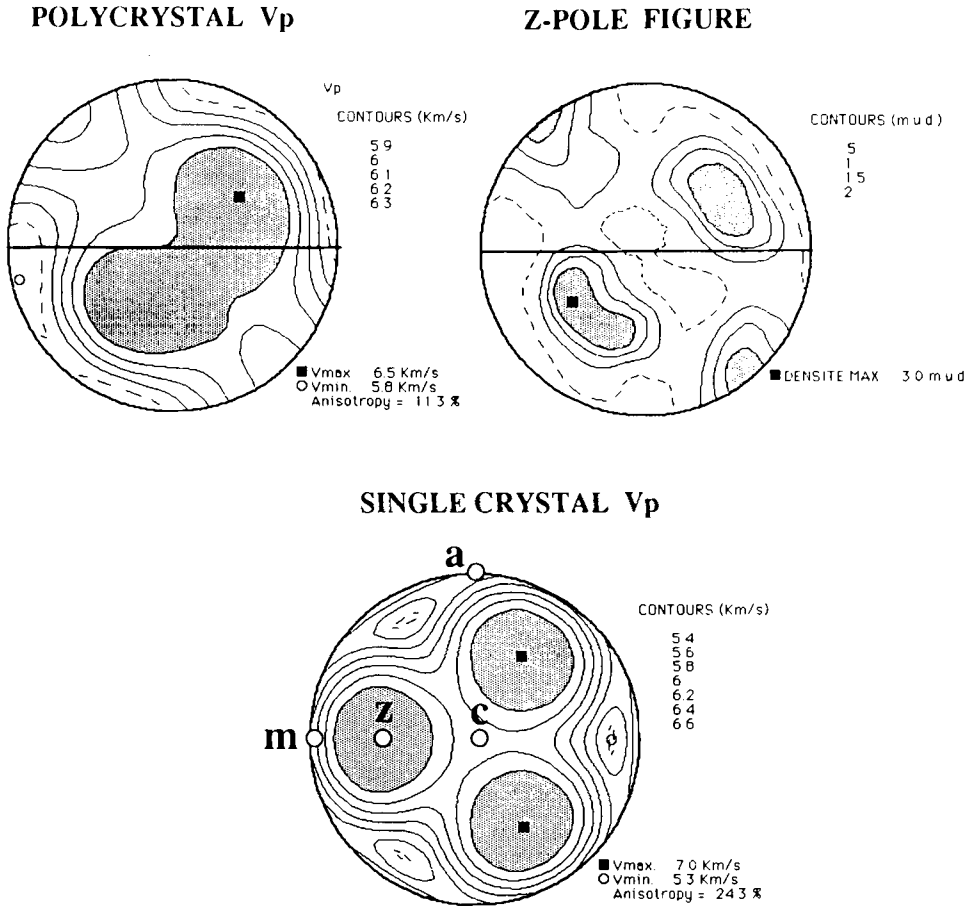

FIG. 9. Variation in seismic P-wave velocities (v_p) with direction, based on the matrix of elastic constants (Table 1) determined from the true ODF. (*a*) P-wave velocities of the Tongue quartzite, contours in km/sec. (*b*) *z*-pole figure, contours in multiples of a uniform density (m.u.d.). (*c*) P-wave velocities for a single crystal of quartz, contours in km/sec.

References

Bunge, H. J. (1982) *Texture Analysis in Materials Science.* Butterworths, London, 593.

—— (1985) Physical properties of polycrystals, and preferred orientation in deformed metals and rocks. In *Preferred orientation in deformed metals and rocks* (H.-R. Wenk, ed.). Academic Press, New York, N.Y., 507–25.

—— and Esling, C. (1986) *Quantitative Texture Analysis.* DGM Informationsgesellschaft Verlag.

Burnham, C. W. (1963*a*) Refinement of the crystal structure of sillimanite. *Zeits. Kristall.*, **118**, 127–48.

—— (1963*b*) Refinement of the crystal structure of kyanite. Ibid., **118**, 337–60.

—— and Buerger, M. J. (1961) Refinement of the crystal structure of andalusite. Ibid., **115**, 269–90.

Chritianssen, F. G. (1986) Deformation of chromite: SEM investigations. *Tectonophys.*, **121**, 175–96.

Day, H. W. and Kumin, H. G. (1980) Thermodynamic analysis of the aluminium silicate triple point. *Amer. J. Sci.*, **280**, 265–87.

Dingley, D. J. (1988) On-line microtexture determination using backscatter Kikuchi diffraction in a scanning electron microscope. In *Proc. Eighth Int. Conf. on Textures of Materials* (J. S. Kallend and G. Gottstein, eds.), The Metallurgical Society, 189–94.

—— and Baba-Kishi, K. (1990) Electron backscatter diffraction in the scanning electron microscope. *Microscopy and Analysis,* Issue 17 (May), 35–7.

Donnay, J. D. H. and Le Page, Y. (1978) The vicissitudes of the low-quartz setting or the pitfalls of enantiomorphism. *Acta Cryst.*, **A34**, 584–94.

Doukhan, J.-C., Doukhan, N., Koch, P. S. and Christie, J. M. (1985) Transmission electron microscopy investigation of lattice defects in Al_2SiO_5 polymorphs and plasticity induced polymorphic transformations. *Bull. Mineral.*, **108**, 89–96.

Faivre, G. and Le Goff, J.-J. (1979) Breakdown of

Friedel's Law in the Kikuchi patterns of tellurium. *Acta Crystal.*, **A35**, 604–10.

Ferguson, C. C., Lloyd, G. E. and Knipe, R. J. (1987) Fracture mechanics and deformation processes in natural quartz: a combined Vickers indentation, SEM and TEM study. *Can J. Earth Sci.*, **24**, 544–55.

Frondel, C. (1962) *Silica Minerals, Dana's System of Mineralogy*, Vol. 3. Wiley, New York.

Hobbs, B. E. and Heard, H. C. (1986) *Mineral and Rock Deformation: Laboratory Studies—The Paterson Volume.* Amer. Geophys. Un., Geophys. Monogr., **36**, 324.

Humphreys, F. J. (1988) Experimental techniques for microtexture determination. In *Proc. Eighth Int. Conf. on Textures of Materials* (J. S. Kallend and G. Gottstein, eds.), The Metallurgical Society, 171–82.

Kallend, J. S. and Gottstein, G. (1988) *ICOTOM: Eighth International Conference on Textures of Materials*, The Metallurgical Society, Warrendale, Pennsylvania, U.S.A., 1127.

Kerrick, D. M. (1990) The Al_2SiO_5 polymorphs. *Reviews in Mineralogy*, **22**, Mineralogical Society of America, Washington D.C.

Lloyd, G. E. (1987) Atomic number and crystallographic contrast images with the SEM: a review of backscattered electron techniques. *Mineral. Mag.*, **51**, 3–19.

—— and Ferguson, C. C. (1986) A spherical electron channelling pattern map for use in quartz petrofabric analysis. *J. Struct. Geol.*, **8**, 517–26.

—— and Knipe, R. J. (1990) Deformation mechanisms active during faulting of quartz upper crustal rocks. Ibid., in press.

—— Ferguson, C. C. and Law, R. D. (1987*a*) Discriminatory petrofabric analysis of quartz rocks using SEM electron channelling. *Tectonophys.*, **135**, 243–9.

—— Law, R. D. and Schmid, S. M. (1987*b*) A spherical electron channelling pattern map for use in quartz petrofabric analysis: correction and verification. *J. Struct. Geol.*, **9**, 251–3.

Mainprice, D. (1990) A FORTRAN program to calculate seismic anisotropy from lattice preferred orientation of minerals. *Computers & Geosciencies*, **16**, 385–93.

Olesen, N. O. and Schmidt, N. H. (1990) The SEM/ECP technique applied on twinned quartz crystals. In *Deformation Mechanisms, Rheology and Tectonics* (R. J. Knipe and E. H. Rutter, eds.), Geological Society of London Special Publication, 369–74.

Pearson, W. B. (1962) *Structure Reports for 1962*, 707–11.

Putnis, A. and McConnell, J. D. C. (1980) *Principles of Mineral Behaviour.* Elsevier, New York.

Rao, C. N. R. and Rao, K. J. (1978) *Phase Transformations in Solids.* McGraw Hill, New York.

Sander, B. (1970) *An Introduction to the Study of Fabrics of Geological Bodies.* English translation, Pergamon Press, Oxford, 641.

Schmidt, N. H. and Olesen, N. O. (1989) Computer-aided determination of crystal-lattice orientation from electron-channeling patterns in the SEM. *Canad. Mineral.*, **27**, 15–22.

Smythe, J. R. and Bish, D. L. (1988) *Crystal Structures and Cation Sites of the Rock-Forming Minerals.* Allen & Unwin.

Vaughan, M. T. and Weidner, D. J. (1978) The relationship of elasticity and crystal structure in andalusite and sillimanite. *Phys. Chem. Minerals.*, **3**, 133–44.

Venables, J. A. and Harland, C. J. (1973) Electron backscattering patterns. *Phil. Mag.*, **27**, 1193–200.

Wenk, H.-R. (1985) *Preferred Orientation in Deformed Metals and Rocks: An Introduction to Modern Texture Analysis.* Academic Press.

—— Bunge, H. J., Kallend, J. S., Lucke, K., Matthies, S., Pospiech, J. and Van Houtte, P. (1988*a*) Orientation distributions: representation and determination. In *Proc. Eighth Int. Conf. on Textures of Materials* (J. S. Kallend and G. Gottstein, eds.), The Metallurgical Society, 17–30.

—— Johnson, G. C. and Matties, S. (1988*b*) Direct determination of physical properties from continuous orientation distributions. *J. Appl. Phys.*, **63**, 2876–9.

Winters, J. K. and Ghose, S. (1979) Thermal expansion and high-temperature crystal chemistry of Al_2SiO_5 polymorphs. *Amer. Mineral.*, **64**, 573–86.

[*Revised manuscript received 4 March 1991*]